29th Congress of the International Council
of the Aeronautical Sciences
St. Petersburg, Russia; September 7-12, 2014

PREDICTED FLIGHT CHARACTERISTICS OF THE INVERTED JOINED WING SCALED DEMONSTRATOR

Mateusz Lis, Adam Dziubiński, Cezary Galiński, Grzegorz Krysztofiak, Paweł Ruchała, Katarzyna Surmacz
Instytut Lotnictwa,

Keywords: *flight performance, flight dynamics, joined wing, simulation*

Abstract

Joined wing configuration is considered as a candidate for future aeroplanes. It is an unconventional aeroplane configuration with several possible advantages like induced drag reduction and weight reduction due to the closed wing concept. This paper presents a predicted flight characteristics of its rarely considered version, with front wing above aft wing. Our previous analyses suggest, that joined wing aeroplane L/D grows together with increasing gap and stagger between wings. This paper presents a summary of flight characteristics explored so far.

Nomenclature

C_D	drag coefficient
C_L	lift coefficient
C_M	pitching moment coefficient
IAS	indicated airspeed
α	angle of attack
β	sideslip angle
ϕ	roll angle
δ_A	aileron deflection
δ_H	elevator deflection
δ_V	rudder deflection
I_x	moment of inertia about X axis
I_y	moment of inertia about Y axis
I_z	moment of inertia about Z axis

1. Introduction

Joined wing configuration is considered as a candidate for future aeroplanes. It is an unconventional aeroplane configuration consisting of two lifting surfaces similar in terms of area and span. One of them is located at the top or above the fuselage, whereas the second is located at the bottom. Moreover one of lifting surfaces is attached in front of aeroplane Centre of Gravity, whereas the second is attached significantly behind it. Both lifting surfaces join each other either directly or with application of wing tip plates, creating a box wing. Application of this concept was proposed for the first time by Prandtl in 1924 [1]. Further development is briefly described in [2 - 4]. It led us to the conclusion that the aeroplane in this configuration should have front wing installed at the top of the fuselage whereas the aft wing should be installed at the bottom of the fuselage [5]. This variant is the opposite to the one frequently presented in the literature [6], however offers very important advantage. Aft wing is far from the front wing wake for all positive angles of attack, which is not the case in the most popular variant of the joined wing designs. Lack of information in the literature about our favourite variant of the joined wing motivated us to organise a research project described in [2 - 4]. Its main purpose

Fig.1 Joined wing demonstrator investigated in this project, in the wind tunnel.

is to understand complex behaviour of the join wing as a strongly aerodynamically coupled [7] configuration. To achieve this goal we are going to test in flight a scaled demonstrator of an aeroplane for four persons, with methods developed in our previous projects [8-11]. Paper [4] presents the design of the demonstrator. Details of its CFD analysis are presented in [12], whereas advanced version of its propulsion system is described in [13]. This paper presents selected flight characteristics obtained from the simulation, based on CFD analysis and wind tunnel tests, with application of methods described in [17, 18]. They are used to prepare the pilot to the flight test campaign.

2. Performance

The most important flight characteristics directly obtainable from the wind tunnel are those related to the aeroplane performance. Figures 2 and 3 show respectively Lift versus Drag polar in trim conditions and gliding ratio as a function of angle of attack. In both cases data are presented for different flaps deflection.

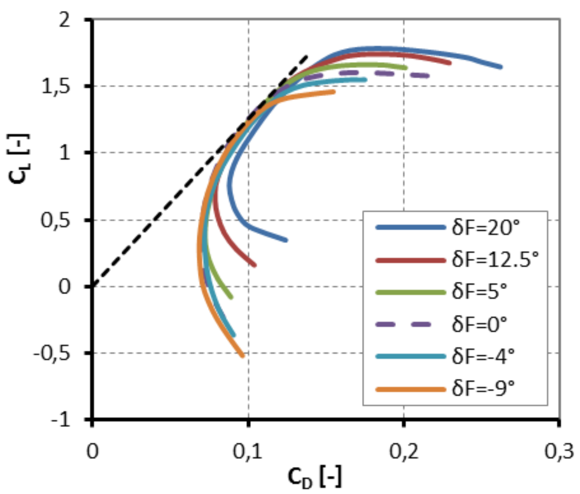

Fig.2 Lift versus Drag polar in trim conditions for various flap deflections and Re=472500. Reference area=the area of the front wing.

As can be seen from these plots relatively high maximum gliding ratio of about 12,5 was achieved as for so low Reynolds number and for an aeroplane with so large fuselage. It should be also mentioned that the model had three-cycle landing gear extended during this measurement. Moreover it also had propeller installed and fixed to simulate the aerodynamic characteristics during real approach to the runway.

Gliding ratio appeared not very sensitive to the flap deflection since the smallest maximum is equal to 11,5 and was achieved for flap deflection as large as 20 degrees. Unfortunately maximum lift coefficient is also not very sensitive to the flaps deflection. Lift coefficient value of 1,8 seems not very small for simple plain flap, but it should be noted that only the area of the front wing was taken as reference area. This area is smaller in the joined wing than in conventional aeroplane with the same total area of lifting surfaces projection at horizontal plane. As a result all coefficients seem to be larger than usually. This is also an explanation for relative large value of the minimum drag coefficient, except of protruding legs of landing gear and propeller blades.

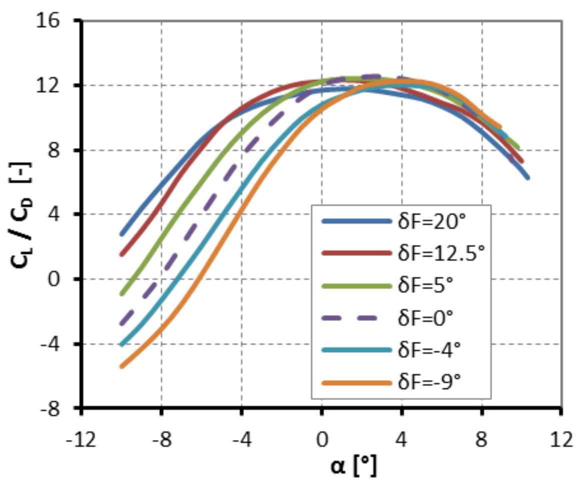

Fig.3 Gliding ratio in trim conditions for various flap deflections and Re=472500.

Even with this condition lift coefficient of maximum gliding ratio is quite large. It is a result of aerodynamic optimization with maximum flight endurance as an objective function. The optimization of presented demonstrator was performed with methods presented in [14-16].

Figure 4 reveals elevator deflections necessary to obtain equilibrium for specific angle of attack and flap deflection. All curves are falling in a monotonic way, which is an indirect prove for longitudinal static stability of the aeroplane.

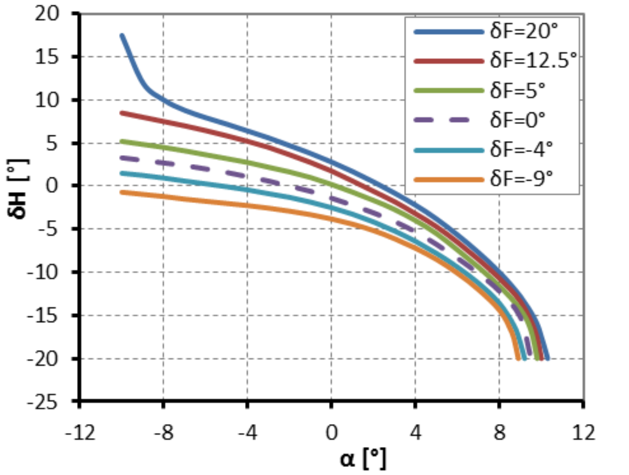

Fig.4 Elevator deflection necessary to obtain equilibrium for deflections and Re=472500.

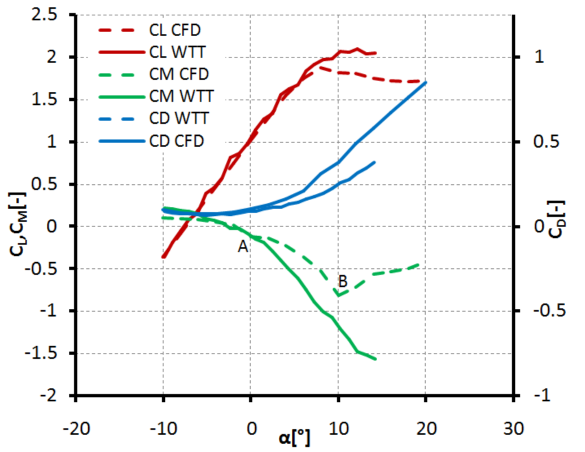

Fig.5 CFD and wind tunnel (WTT) results of lift drag and pitching moment coefficients. Two discontinuities pointed on the figure are the beginning of the separation on front (A) and aft (b) wing.

Comparison between RANS simulation (CFD) performed at the beginning of the project and wind tunnel tests (WTT) in Figure 5 shows two areas (A and B) of visible parameters change, caused by the separation (stall) on wings. Appropriate shear distribution with marked areas of separation has been shown in Figure 6 and Figure 7. Difference between CFD and WTT seems to be a result of the roughness of the wing surface at relatively low Reynolds number. As a conclusion it is recommended to leave the rough top surface of the wing also for the flight tests, as it increases the flight safety by delaying a stall to higher angles of attack, as proved by the experiment.

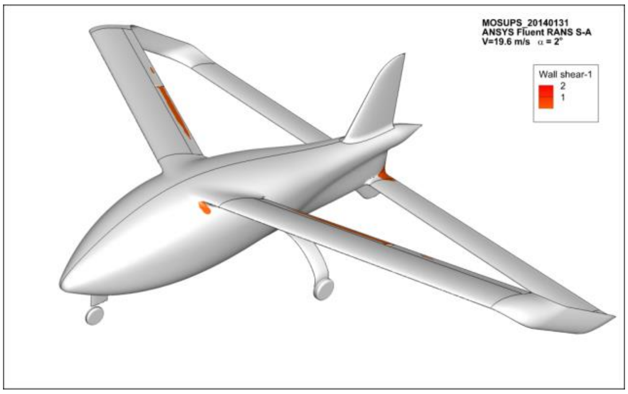

Fig.6 Area of reverse flow (stall) on rear wing marked with orange color. Airspeed = 19.6m/s, AoA = 2°

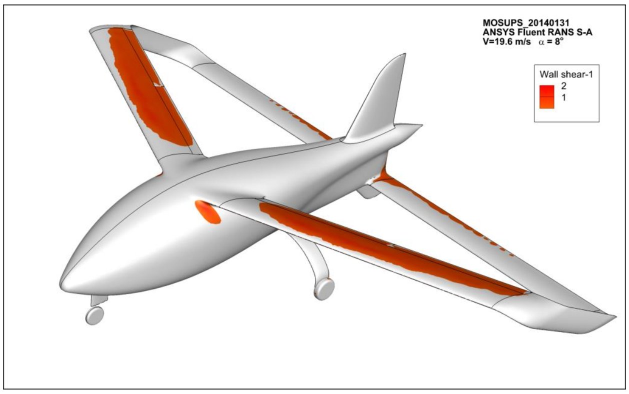

Fig.7 Area of reverse flow (stall) on rear wing marked with orange color. Airspeed = 19.6m/s, AoA = 8°

3. Simulation of dynamic stability

Simulation of dynamic stability for the demonstrator take-off weight of 24,5kg was done with application of SDSA software package, which is described in detail in [17, 18].

Moments of inertia assumed for simulation were the following:

$I_x = 6{,}945$ [kg·m^2]
$I_y = 10{,}102$ [kg·m^2]
$I_z = 15{,}658$ [kg·m^2]

At the beginning of the simulation equilibrium conditions for airspeed of 25 m/s in a propulsion-less flight were defined. Then various disturbances were introduced to observe the dynamic response of the aeroplane. The following disturbances were introduced:

1) excess in angle of attack by 5 degrees (Figure 8)
2) excess in airspeed by 2m/s (Figure 9)
3) pulsed elevator deflection up by 20 degrees within 0,5s (Figure 10)
4) pulsed elevator deflection up and down by 20 degrees within 0,5s (Figure 11)
5) excess in bank angle by 10 degrees (Figure 12)
6) excess in bank angle by 20 degrees (Figure 13)
7) excess in yaw angle by 10 degrees (Figure 14)
8) excess in yaw angle by 20 degrees (Figure 15)
9) pulsed rudder deflection by 20 degrees within 0,5s (Figure 16)
10) pulsed ailerons deflection by 20 degrees within 0,5s (Figure 17)

Data presented in Figures 8-11 show lack of short period oscillations in the response to different disturbations. Moreover phugoid oscillations appeared decreasing progressively. They have period of about 14 s and time to half amplitude of about 16 s. This is a prove of longitudinal static and dynamic stability.

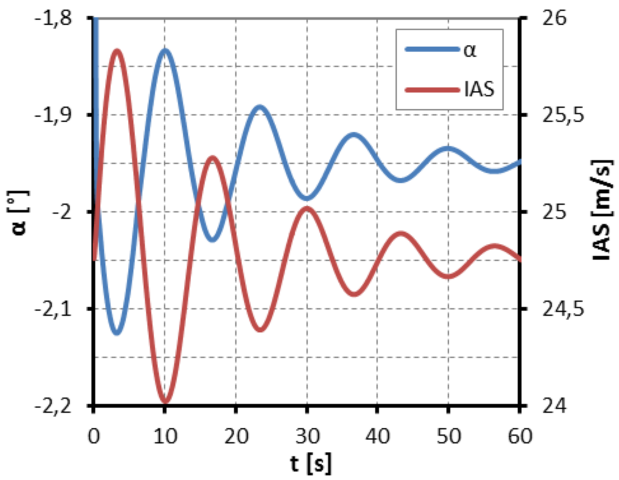

Fig.8 Dynamic response to the excess in angle of attack by 5 degrees.

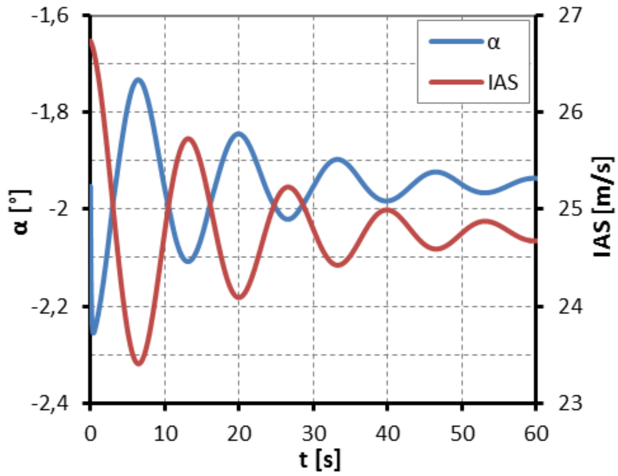

Fig.9 Dynamic response to the excess in airspeed by 2m/s.

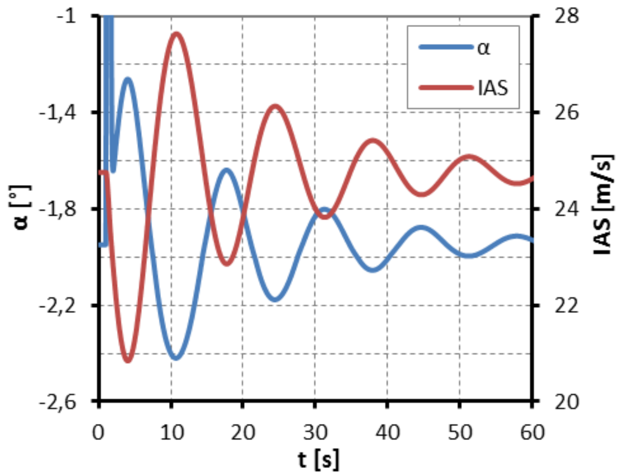

Fig.10 Dynamic response to the pulsed elevator deflection up by 20 degrees within 0,5 s.

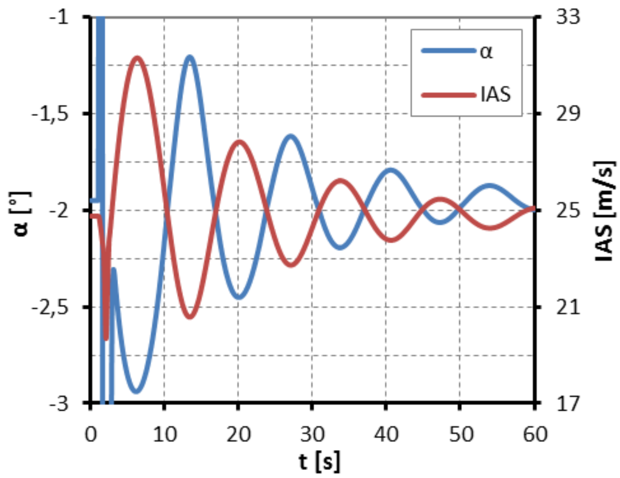

Fig.11 Dynamic response to the pulsed elevator deflection up and down by 20 degrees within 0,5 s.

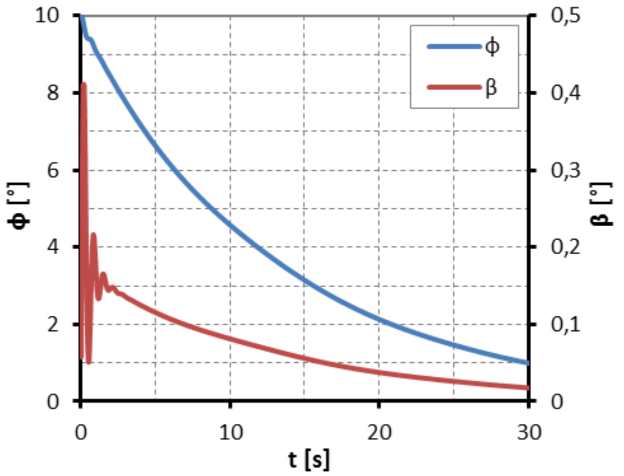

Fig.12 Dynamic response to the excess in bank angle by 10 degrees.

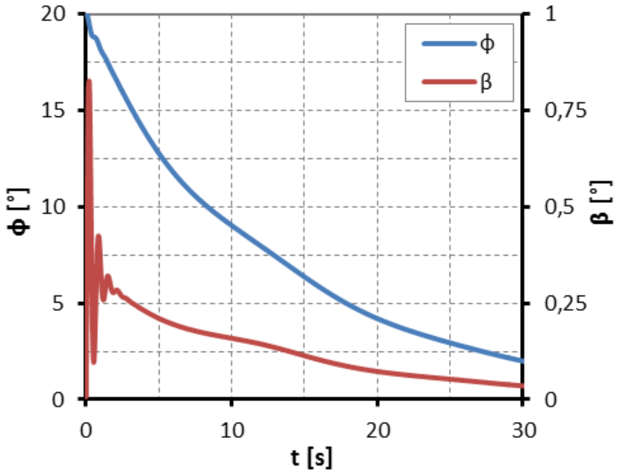

Fig.13 Dynamic response to the excess in bank angle by 20 degrees.

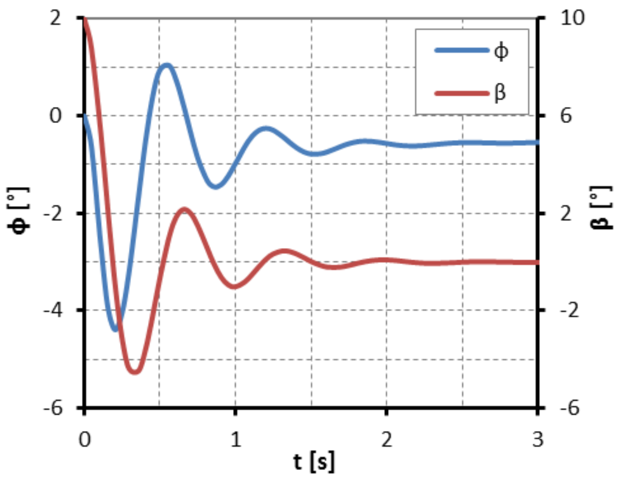

Fig.14 Dynamic response to the excess in yaw angle by 10 degrees.

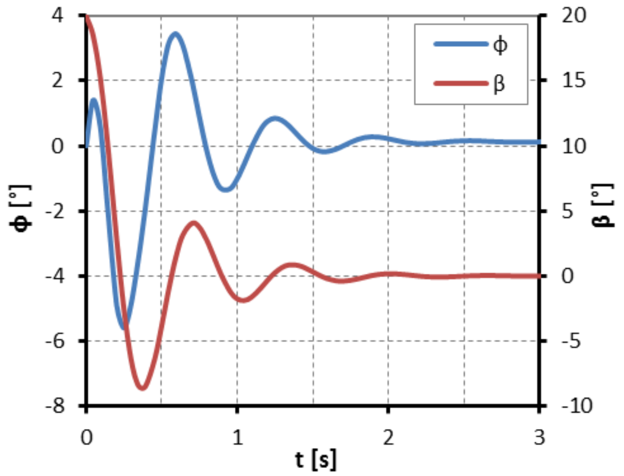

Fig.15 Dynamic response to the excess in yaw angle by 20 degrees.

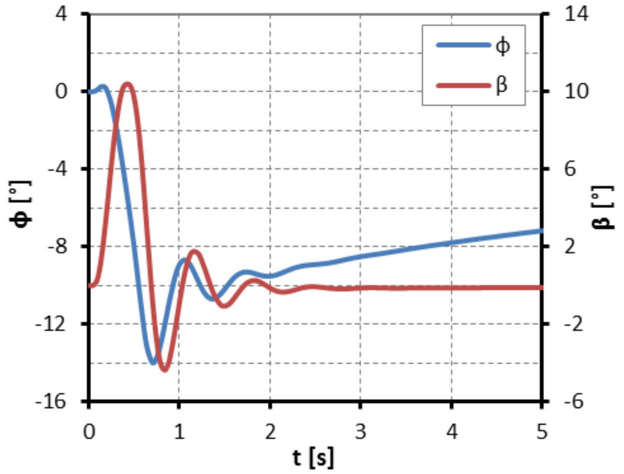

Fig.16 Dynamic response to the pulsed rudder deflection by 20 degrees within 0,5 s.

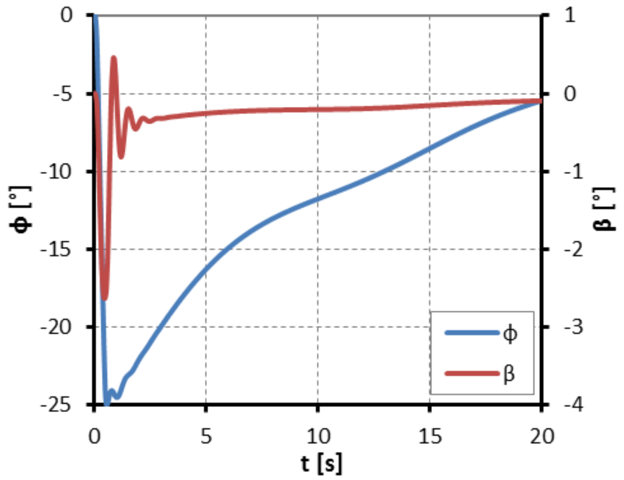

Fig.17 Dynamic response to the pulsed ailerons deflection by 20 degrees within 0,5 s.

In the case of data presented in Figures 12-17 no Dutch-roll instability was observed, which is good for dynamic stability. Similarly, simulation does not show evince of the aeroplane tendency to spiral instability. Simulation results presented in Figures 12, 13, 17 show aeroplane response to lateral disturbations that have been defined as two different initial roll angle and pulsed aileron deflection appropriately. In all these cases time to half amplitude equals about 8 s, that seems to be reasonable for that type of the aeroplane. Results presented in Figures 14-16 reveal very strong directional stability. After disturbation in yaw angle or pulsed rudder deflection, oscillations with period of about 0,6 s are induced. These oscillations are completely damped and within 2 s. What is worth to mention about is that whilst yaw angle oscillates about the neutral position and is heavily damped in very short time, bank angle tends to decrease steadily in significantly longer period. It can be suspected that this property is caused by specific aeroplane geometry, i.e. additional plates at wing tips, that give effect similar to vertical stabilizer increasing directional stability.

4. Aeroplane response to controls deflections

As shown above, aeroplane presents satisfactory stability qualities. To fully assess aeroplane characteristics, it was decided to perform maneuverability analysis to define whether aeroplane response to control surfaces deflections is correct and allows to recover the aeroplane from undesired states. According to certification specifications, two tests for rate of roll have been performed. Both of them aimed at simulating roll rate form steady 30 degrees banked turn to the opposite 30 degrees turn after full aileron deflection. The indicator of controllability for this trial is time required to reverse the direction of the turn. The first test was performed for aeroplane approach in landing conditions, i.e. flaps fully extended, engine operating at idle and airspeed equal $1{,}3 \cdot V_{S1}$. Results can be observed in Figure 18.

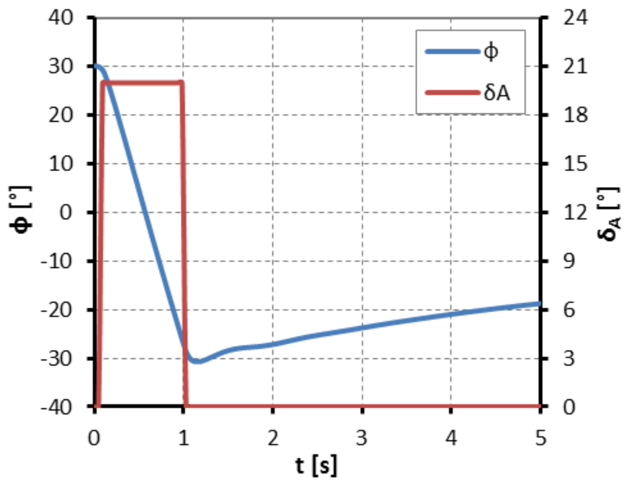

Fig.18 Standard roll rate test for aeroplane approach for landing condition.

The second test performed to evaluate roll controllability was intended for climbing stage just after take-off. Initial conditions were: flaps in a take-off position, maximum engine power and airspeed equal $1{,}2 \cdot V_{S1}$.

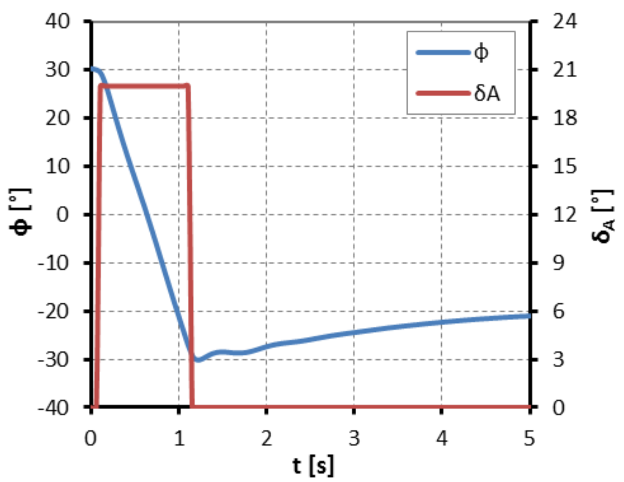

Fig.19 Standard roll rate test for aeroplane climbing stage condition.

Figures 18-19 show that in both considered flight stages aeroplane response is fast, robust and compliant with expectations, so that it should be possible to control it in these states. Time to reverse the turn is about 1 s and 1,2 s for landing and climbing stages appropriately. These values are much lower than maximum allowed in regulations, what means that the aeroplane meets lateral controllability requirements, moreover there is some reserve for emergency cases.

Another simulation that was performed aimed at assessing flaps deflection influence on longitudinal stability, which is crucial especially during approach and landing phase. Two deflection values were investigated: 10 and 20 degrees down. Results can be seen in Figures 20-21. Figures show that for both deflection values, oscillations decrease moderately. Time constant for oscillations on the first figure equals about 10 s, while on the latter about 9 s. Oscillations magnitude is very low and additionally time to half amplitude equals about 10 s in the first and the latter case, which means flaps pose no danger to longitudinal stability.

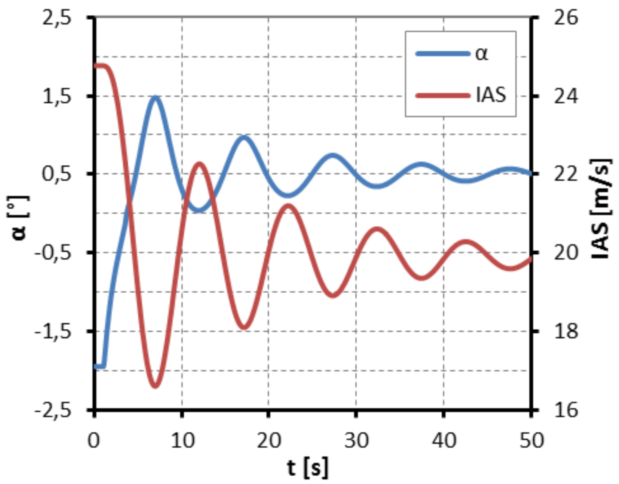

Fig.20 Dynamic response to flap deflection by 10 degrees down.

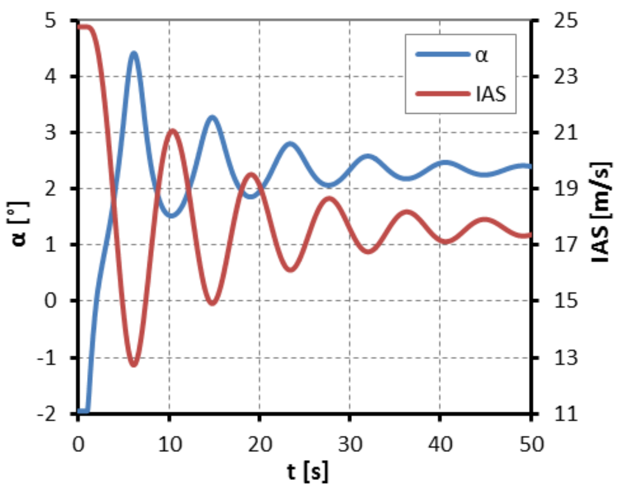

Fig.21 Dynamic response to flap deflection by 20 degrees down.

Determination of propulsion unit impact on stability was the last type of analyses performed to assess aeroplane flight qualities. Several cases were simulated for this purpose. No gyroscopic effects and propeller torque effect were taken into account during these analyses, so the only factor that generated disturbances was a pitching moment due to thrust. In all of the simulations described below aeroplane was trimmed for initial conditions but no controls deflections were introduced during simulation after disturbance occurred (thrust change). The first two cases which results are shown in Figure 22-23, aimed at evaluating airplane response to rapid thrust increase from 0 to 100% that is typical situation for go-around procedure. Two cases were investigated: without flap extended and with flap in landing position. Longitudinal oscillation was indicated as a result with time constant of about 14 s and time to half amplitude about 15 s.

It was also decided to investigate aeroplane behavior in situation when throttle is shut from 100 to 0%. This reflects situation when engine fails, i.e. during climbing stage after take-off. So that it is very important from the safety reasons to predict how the aeroplane will react and how to control it in that case. As previously, two cases were investigated: without flap extended and with flap in take-off position. Results are presented in Figures 24-25.

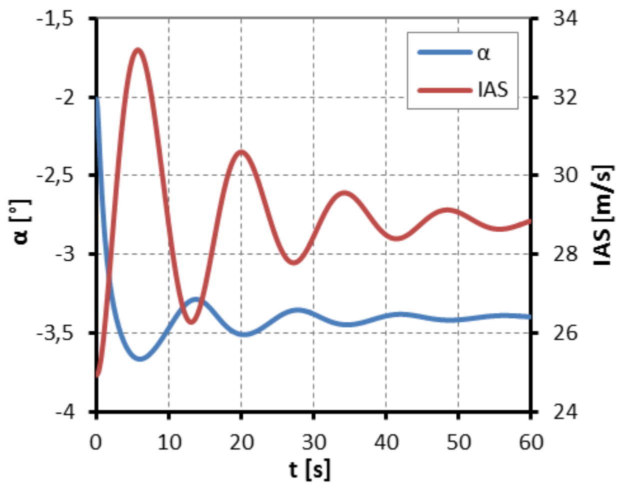

Fig.22 Dynamic response to rapid, full throttle opening. No flap extended.

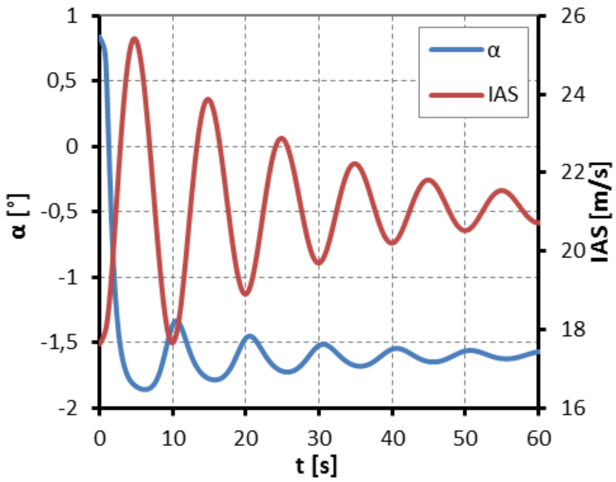

Fig.23 Dynamic response to rapid, full throttle opening. Flap fully extended.

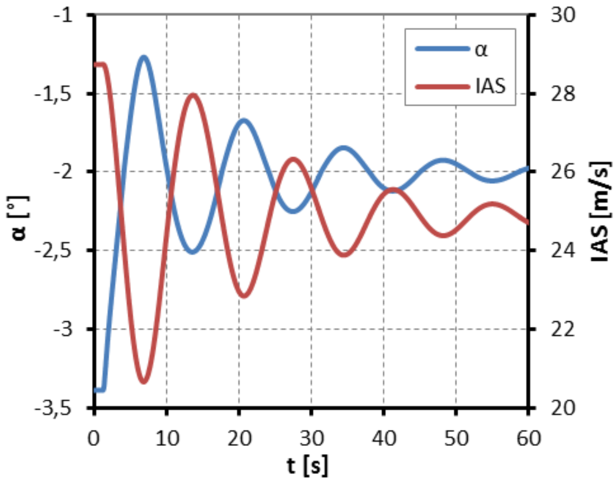

Fig.24 Dynamic response to throttle cut-off. No flap extended.

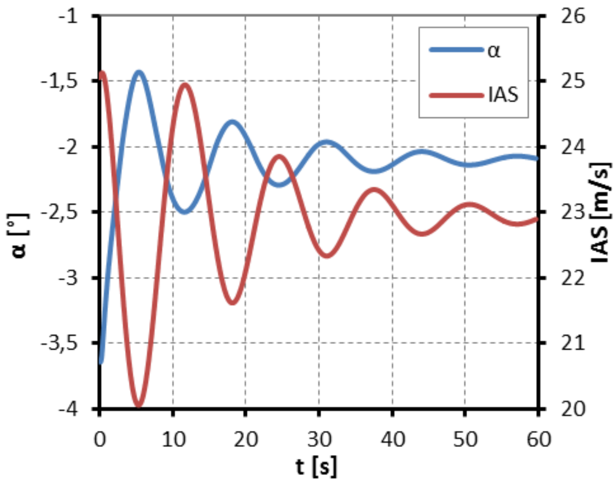

Fig.25 Dynamic response to throttle cut-off. Flap in take-off position.

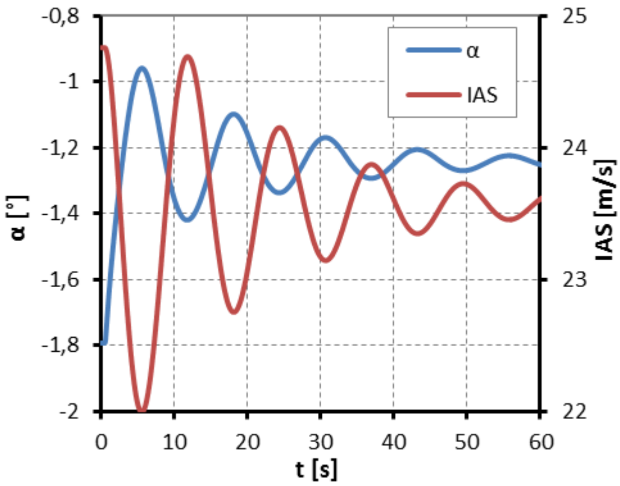

Fig.26 Dynamic response to throttle reduction from 72% to 0%. No flap extended.

After sudden throttle shut down, aeroplane tends to oscillate with time constant of about 15s for configuration without flap extended and about 13 s with flap in take-off position. Time to half amplitude equals about 10 s in both cases.

The last analysis described herein is simulation of aeroplane response to throttle reduction from 72% (nominal throttle required for steady horizontal flight) to 0%. It was assumed that controls are frozen all along, so the pitching effect presented in Figure 25 arises directly from thrust change. It shows that after trust reduction, oscillations are similar to the other, previously presented. Amplitude is not significant and decreases progressively, so that no input from pilot is essential to hold the aeroplane in stable flight.

5. Conclusion

Simulation of flight characteristics was performed for the joined wing flying demonstrator, to check if its flight test campaign can be safely performed. Aeroplane exhibited longitudinal static stability as well as dynamic stability. Neither Dutch roll nor spiral modes appeared divergent within the most interesting range of airspeeds. Every oscillations generated by state disturbance or controls deflections are convergent in reasonable time with small time to half amplitude. Aeroplane response to controls deflections and thrust change are predictable and correct. In none of the analyzed cases dangerous situation was observed. That suggests aeroplane airworthiness. Low Reynolds number effects are a major concern.

6. Acknoledgements

This work was supported by The National Centre for Research and Development under grant No. PBS/A6/14/2012. Special thanks to the all personel of MSP company who manufactured the model and to the all personnel of the wind tunnel facility, who performed the experiment.

References

[1] Prandtl, L., ñInduced drag of multiplanesò, NACA TN 182, 1924.

[2] Galinski C., Hajduk J., ñAssumptions of the Joined Wing Flying Model Programmeò, *Transactions of the Institute of Aviation*, in print.

[3] Galinski C., Hajduk J., Kalinowski M., SeneŒko K., ĂThe Concept of the Joined Wing Scaled Demonstrator Programmeò, Proceedings of the CEASô2013 conference, CEAS, Linkoping, Sweden, 2013, pp. 244-253, URL: http://www.ceas2013.org/images/images/CEAS2013.pdf [cited 05 April 2014].

[4] GaliŒski C., Hajduk J., Kalinowski M., Wichulski M., Stefanek Ğ. ĂIverted Joined Wing Scaled Demonstrator Programmeò, Proceedings of the ICASô2014 conference, ICAS, Petersburg, Russia, 2014, ICAS2014-P2.4.13, in print

[5] Mamla P., Galinski C., ñBasic Induced Drag Study of the Joined-Wing Aircraftò, *Journal of Aircraft*, Vol. 46, No. 4, 2009, pp. 1438-1440.

[6] Wolkovitch, J., ĂThe joined wing - An overviewò, *Journal of Aircraft*, Vol. 23, No. 3, 1986, pp. 161-178.

[7] Goraj Z., Kulicki P., Lasek M., ĂAircraft Stability Analysis For Strongly Coupled Aerodynamic Configurationò, *Journal of Theoretical and Applied Mechanics*, Vol. 35, No. 1, 1997, pp.137-158.

[8] GaliŒski C., Bartkiewicz P., Hajduk J., Lamers P., ñResults of the J-5 Marco Dynamic Similar Model Flight Tests Programò, SAE Paper No. 975551, 1997.

[9] Goraj Z., Szender M., ĂBadania modelu samolotu w locie na duŨych kŃtach natarciaò, Proceedings of VI Konferencja "Metody i Technika BadaŒ Statków Powietrznych w Locie", ITWL, MrŃgowo, Poland, 2004, pp. 143-153.

[10] Goraj Z., Szender M., ñTechniques and critical technologies applied for small and mini UAVs. State of the art and development perspectivesò, *Transactions of the Institute of Aviation*, No. 183, 2005, pp. 41-49.

[11] Goraj Z., Kittmann K., Voit-Nitschmann R., Szender M., ñDesign and Integration of Flexi-Bird - a Low Cost Sub-Scale Research Aircraft for Safety and Environmental Issuesò, Proceedings of the ICAS Congress 2012, ICAS, Brisbane, Australia, 2012, URL: http://www.icas.org/ICAS_ARCHIVE/ICAS2010/ABSTRACTS/469.HTM [cited 20 April 2014].

[12] DziubiŒski A., Kuprianowicz S., Surmacz K., GaliŒski C., Ģóğak J., ĂThe Joined Wing Scaled Demonstrator Results of CFD Analysisò, Proceedings of the ICASô2014 conference, ICAS, Petersburg, Russia, 2014, ICAS2014-1.10ST, in print.

[13] BogdaŒski K.; Rodzewicz M., Krusz W.; Rutkowski M.; ĂDesign and Optimization of Low Speed Ducted Fan for a New Generation of Joined Wing Aircraftò, Proceedings of the ICASô2014 conference, ICAS, Petersburg, Russia, 2014, ICAS2014-P2.4.13, in print

[14] Stalewski W., "Parametric Modelling of Aerodynamic Objects - The Key to Successful Design and Optimisation", *Aerotecnica Missili e Spazio*, Vol. 91, No. 1/2, 2012, pp. 23-31, URL: http://citeseerx.ist.psu.edu/viewdoc/download?doi=10.1.1.306.9906&rep=rep1&type=pdf [cited 20 April 2014].

[15] Stalewski W., Ģóğak J., ñOptimisation of the helicopter Fuselage with Simulation of Main and Tail Rotor Influenceò, Proceedings of the ICAS Congress 2012, ICAS, Brisbane, Australia, 2012, URL: http://www.icas.org/ICAS_ARCHIVE/ICAS2012/ABSTRACTS/811.HTM [cited 20 April 2014].

[16] Stalewski W., Ģóğak J., ñMulti-objective and Multidisciplinary Optimization of Wing for Small Aircraftò, Proceedings of the CEAS Congress on disc [CD-ROM], Venice, Italy, 2011, pp. 1483-1492.

[17] Goetzendorf-Grabowski T.; Mieszalski D.; Marcinkiewicz E.; ñStability analysis using SDSA toolò, *Progress in Aerospace Sciences*, Volume 47, Issue 8, 2011, pp. 636-646

[18] Goraj Z. ñFlight dynamics models used in different national and international projectsò, *Aircraft Engineering and Aerospace Technology*, Volume 86, issue 3, 2014, pp.166-178

Copyright Statement